Numerical and experimental study of cellular structures as a heat dissipation media

Ahmed Tariq, H., Israr, A., Khan, Y. I. & Anwar, M.

Original citation & hyperlink:
Ahmed Tariq, H, Israr, A, Khan, YI & Anwar, M 2019, 'Numerical and experimental study of cellular structures as a heat dissipation media' Heat and Mass Transfer, vol. 55, no. 2, pp. 501–511.
https://dx.doi.org/10.1007/s00231-018-2439-7

DOI 10.1007/s00231-018-2439-7
ISSN 0947-7411
ESSN 1432-1181
Publisher: Springer

The final publication is available at Springer via http://dx.doi.org/10.1007/s00231-018-2439-7

NUMERICAL AND EXPERIMENTAL STUDY OF CELLULAR STRUCTURES AS A HEAT DISSIPATION MEDIA

Hussain Ahmed Tariq[1*]

Department of Mechanical Engineering, Institute of Space Technology, Islamabad, Pakistan

ahmedtariq90@gmail.com

+923455333219

Asif Israr[2]

Department of Mechanical Engineering, Institute of Space Technology, Islamabad, Pakistan

asif.israr@ist.edu.pk

Yasir Imtiaz Khan[3]

School of Computing, Electronics and Maths, Coventry University, United Kingdom

ac4704@coventry.ac.uk

Muhammad Anwar[4]

Department of Mechanical Engineering, Institute of Space Technology, Islamabad, Pakistan

Faculty of Sciences, The University of Nottingham, United Kingdom

manwar18@gmail.com

*corresponding author

ABSTRACT

High heat fluxes generation in electronic devices demands new modes, methods and structures to dissipate the generated heat effectively. In this work, we investigate the thermal performance of cellular structures using computational fluid dynamics (CFD) and report an optimal cellular structure for effective heat dissipation. We validate our numerical results with experimental results obtained using optimized cellular structure. We find the minimum base temperature for the optimized cellular structure to be 43.6^{0}C and 47.4^{0}C numerically and experimentally respectively with inlet velocity of 10m/s and heat flux of 35503W/m^2. The numerical results for the base temperature are in close agreement with experimental results with an error of 8.71%. Previously the base temperatures using air with inlet velocity of 11.1m/s and water with inlet velocity of 1.03m/s have been reported to be 55^{0}C and 40.5^{0}C respectively [1] and [2].

KEYWORDS: Thermal management index, pressure loss coefficient, squarebore microhole, base temperature.

NOMENCLATURE

A_b	= Frontal blocked area
A_t	= Frontal total area
A_s	= Surface Area
b	= Length of square side
c	= Centre to centre distance
C_p	= Specific heat
d	= Bore diameter
D_h	= Hydraulic diameter
d_h	= Hole diameter
H	= Height
K_{cell}	= Pressure loss coefficient
L	= Length
$\dot{m}$	= Mass flow rate
ΔP	= Pressure Difference
$\dot{Q}$	= Heat transfer rate
R_{BR}	= Blockage ratio
R_{OPEN}	= Open area ratio
T_b	= Base temperature
T_i	= Inlet Temperature of air
T_o	= Outlet Temperature of air
t	= Wall thickness
v_i	= Inlet velocity
v_o	= Outlet velocity
V	= Volume of the structure
V_b	= Total volume of whole solid block
W	= Width

Greek symbol

α_{sf}	= Surface area density
ε	= Porosity
η	= Thermal management index

1. INTRODUCTION

Electronic devices have become a very essential part in our daily lives. The continuous generation of heat fluxes in the electronic devices should be removed continuously to maintain the base temperature of the device in a safe zone. Pin fin array heat exchange method is becoming insufficient to meet the high heat transfer requirements in electronics. One of the techniques which have been used by many researchers is to increase the heat transfer rate by increasing the surface to volume ratio of heat sink devices. They provide higher surface area densities as compared to the conventional methods, which allow a dynamic mixing between the flowing fluid and the internal structure. As a result, the convection between the solid and fluid is enhanced.

New techniques are under discussion for effective thermal management and to maintain the base temperature of the computer processors in a safe zone which is between 60^o and 80^{o}C. It has been reported that the heat dissipation of desktop and mobile processors are 100W and 30W, respectively. [3]. The thermal performance of air cooled mini channel heat sinks with different configurations have been investigated experimentally and it has been observed that the heat transfer to air from solid increases with increasing flow rate and base temperature. The base temperature has been reported to be 55ºC at the inlet velocity of 11.1m/s and heat generation of 160W. [1]

Cellular metal structures are ultra-light materials with high porosities. In past few years they have been emerged as a compact heat exchanger to dissipate heat in small spaces [4] [5]. It is evident from previous research work that the heat transfer performance of aluminium foam heat sinks is better than that of conventional pin finned and parallel plate heat sinks [6-9].

Cellular metallic foams with stochastic structure are used as a compact heat exchanger. Metal foam has the ability to endorse eddies and mixes the coolant fluid efficiently which enables it to remove heat five times faster than conventional pin fin array while having three time lesser weight.[10-14]. Metal foam offers unique thermal, mechanical and electrical properties at relatively low density. Several heat transfer characteristics of metal foams have been investigated including the effect of microstructure properties such as porosity, relative density, pore density, pore size, ligament diameter, and permeability. [15-19]

Overall reliability and operating speed of the modern high speed computers depends not only on the base temperature but also on the temperature uniformity over the surface. Therefore, cellular periodic structures are preferred over stochastic structures (metal foams) which are able to provide a uniform temperature distribution over the surface. Stochastic cellular structures are good in dissipating heat as compared to periodic cellular structures but their load bearing capability is much inferior than periodic cellular structure. [6]

It has been observed that the thermal efficiency of the brazed textile structures (cellular periodic structure) of forced air convection was approximately three times larger than that of open-celled metal foams (cellular stochastic structure). The surface to volume ratio provided by metal foams is higher but pressure drop of periodic textile structure is lesser than the pressure drop in metal foams. In this case, heat is not dissipating through heat convection only but heat conduction also plays an important role in dissipating the heat along with the convection. A good heat exchanger actually dissipate the generated heat flux at higher rate with a very low pumping power which is required to overcome the pressure drop to move the coolant through the heat exchanger. Thermal management of any heat sink/heat exchanger can be computed by the ratio of heat transfer rate to pressure drop. [7]

A study was made to cool the processor temperature using nanofluids. The largest temperature drop from 49.4ºC to 43.9ºC was observed using alumina nanofluid for 1% of volumetric concentration at a flow rate of 1L/min when compared with the pure base fluid. [8]. For effective thermal management of high heat flux generating microprocessors, five different geometries with different fin spacing have been tested using water as a coolant. It is experimentally investigated that the heat sink with pin spacing of 0.2mm drops the base temperature of the microprocessor up to 40.5ºC at a heater power of 325W. [2]

In this research, 2-D void arrangement particularly from one side square and the other with circular cross section is not addressed yet. Moreover a comparison of cellular structures with 2-D void arrangement circularbore structures, 2-D and 3-D void arrangement squarebore structures are discussed in details. Numerical study is evaluated on different cellular structures and optimized structure is than validated with experimental results.

2. NUMERICAL ANALYSIS

The computational fluid dynamics (CFD) approach is used to stimulate the conjugate heat transfer problem. We gave analyse different cellular structure designs using commercial CFD software package. We have used ANSYS design modeller for modelling, ANSYS meshing for CFD meshing and ANSYS fluent as a CFD solver. We find and present an optimal cellular structure for heat dissipation on the basis of these simulations.

2.1. Boundary conditions

The following boundary conditions are imposed:-

- Heat supplied of 150W at the bottom surface
- Flow inlet velocity at 6m/s
- Pressure outlet at 0 gauge pressure
- Insulated boundary condition is imposed to the top and on two side walls
- Air is coming in at the temperature of 25^0C

2.2. Data Reduction

We adopt following procedure for data reduction for all the structures.

Heat removed by the air circulating in the structure can be calculated from (1) by applying conservation principle with one inlet and one outlet and assuming negligible changes in kinetic and potential energies as:-

$$\dot{Q} = \dot{m}C_p(T_o\text{-}T_i) \tag{1}$$

Porosity can be calculated from (2)

$$\varepsilon = 1\text{-}(V/V_b) \tag{2}$$

Blockage ratio and open area ratio can be calculated from (3) and (4)

$$R_{BR} = A_b/A_t \tag{3}$$

$$R_{OPEN} = (1\text{-}\ R_{BR}) \tag{4}$$

Pressure loss coefficient can be calculated from (5)

$$K_{cell} = \left(\frac{1-R_{OPEN}}{R_{OPEN}}\right)^2 \tag{5}$$

Surface area density can be calculated from (6)

$$\alpha_{sf} = A_s/V \tag{6}$$

Thermal management index can be calculated from (7)

$$\eta = \dot{Q}/\Delta P \tag{7}$$

2.3. Parametric Study

A parametric study is carried out to find the optimized cellular structure. In this process, we vary only one parameter and keep all of the other parameters constant. We initially select Copper as structure material. Following sequence is followed for the parametric study:-

- Effect of Bore Diameter
- Effect of Design
- Effect of Height
- Effect of Material

2.3.1. Effect of Bore Diameter

We study the effects of bore diameter on of different structures on the heat transfer. We present details of these structures show in Table 1, while keeping all the other parameters (H, W, L, and t) constant and find the optimum bore diameter. All the circular bore structures have void arrangement along x and z axis. We show one of the cellular structures in the Fig. 1. We compare the results for three structures in Table 2.

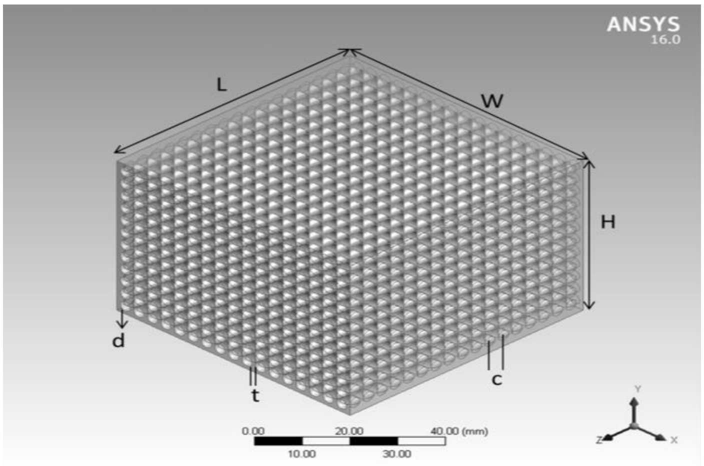

Fig. 1 Cellular structure; circularbore1

Table 1 Cellular structures dimension (mm)

	Circularbore1	Circularbore2	Circularbore3
d	3	4	5
c	4	5	6
t	1	1	1
H	48.5	48.5	49
L	69	69	67
W	69	69	67

Table 2 Effect of bore diameter

	Circularbore1 (Cu)	Circularbore2 (Cu)	Circularbore3 (Cu)
T_b (^{0}C)	47.7	60	66.2
ΔP (Pa)	445.6	305.4	196.1
$\dot{Q}$ (W)	117.1	80.4	48.4
ε	0.58	0.63	0.67
R_{BR}	0.57	0.51	0.47
R_{OPEN}	0.43	0.49	0.53
α_{sf} (1/m)	1486.7	1404.2	1331
η (m^3/s)	0.26	0.26	0.24

In Table 2, it can be seen that the thermal management index (η) of the three structures is almost the same. It can also be seen from Table 2 that the circularbore1 shows lowest base temperature and maximum heat transfer compare to the other two structures. Therefore, we select bore diameter of 3mm for the further study.

2.3.2. Effect of Design

In order to study the effect of different designs, we use the squarebore of dimensions 3mm×3mm and compare the results with already selected 3mm bore diameter of circularbore1 structure. As in previous section, d is selected as 3mm, so b is also selected as 3mm in further study. All the parameters (H, W, L, t, and b) will be fixed in the further study, while structure designs will be varied. Squarebore1 has square void arrangement along x,y,z axis, squarebore2 has square void arrangement along x and z axis while squarebore3, squarebore microhole1 and sqaurebore microhole2 has square void arrangement along y and z axis. We present details of these structures show in Table 3.

Table 3 Cellular structures dimension (mm)

	Squarebore1	Squarebore 2	Squarebore 3	Squarebore microhole1	Squarebore microhole2
b	3	3	3	3	3
t	1	1	1	1	1
d_h	-	-	-	2	1.5
c	-	-	-	4	4
H	49	49	49	49	49
L	65	65	65	65	65
W	65	65	65	65	65

Table 4 Effect of design

	Squarebore1 (Cu)	Squarebore2 (Cu)	Squarebore3 (Cu)	Squarebore microhole1 (Cu)	Squarebore microhole2 (Cu)
T_b (^{0}C)	62.4	53.7	46.6	46.7	46.2
ΔP (Pa)	360.8	256.1	254.1	175.1	163.1
$\dot{Q}$ (W)	112.8	83.2	94.1	98.7	111
ε	0.80	0.67	0.67	0.59	0.57
R_{BR}	0.45	0.45	0.45	0.45	0.45
R_{OPEN}	0.55	0.55	0.55	0.55	0.55
α_{sf} (1/m)	2914	2029	2018	1827	1786
η (m^3/s)	0.31	0.32	0.37	0.56	0.66

We show results for five different designs (squarebore1, squarebore2, squarebore3, squarebore microhole1 and squarebore microhole2) in Table 4. It can be seen that all the squarebore structures are offering higher efficiency as compare to circularbore structures discussed in previous section. Squarebore1 and squarebore microhole2 structures are dissipating maximum heat among all structures but there is a less pressure drop in squarebore microhole 2 structure. Therefore, squarebore microhole2 have the highest thermal management index as compare to the other structures. Squarebore microhole2 structure is selected as the final design for the further study.

2.3.3. Effect of Height

Optimum height for the selected design will be chosen in this section. Temperature variation with the height can be seen in the plot between temperature and height in the Fig. 2. After certain height, the temperature is not changing considerably and the curve almost becomes flat, so 0.037m is selected as an optimum height.

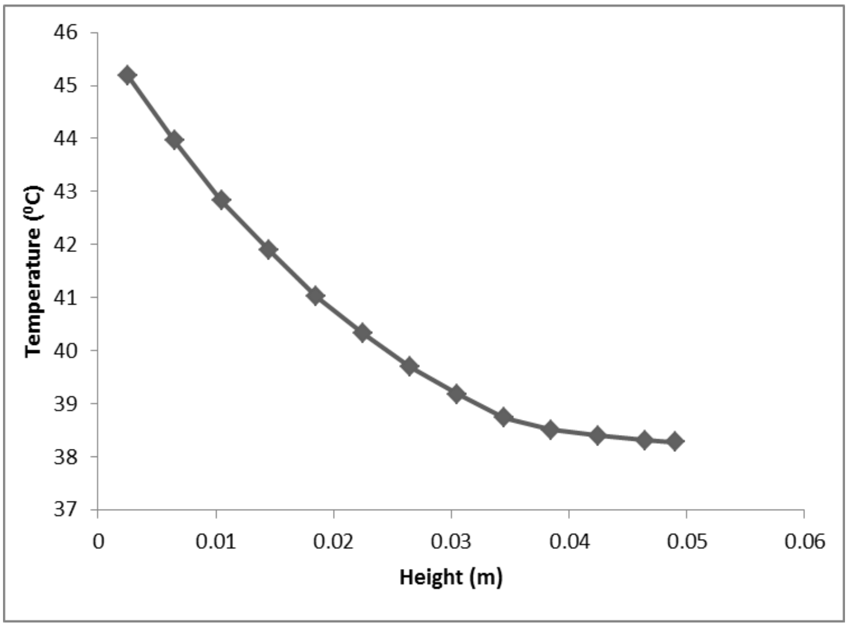

Fig. 2 Effect of temperature with height

2.3.4. Effect of Material

We find that the squarebore microhole3 is the optimal structure from the investigated structures with height of 37mm. We used Copper material for the cellular structures till now, now we compare the results for Copper and Aluminum in Table 5.

Table 5 Effect of material

	Squarebore microhole3 (Cu)	Squarebore microhole3 (Al)
T_b (^{0}C)	49.7	54
ΔP (Pa)	166.4	163.5
$\dot{Q}$ (W)	99.2	88.4
ε	0.57	0.57
R_{BR}	0.46	0.46
R_{OPEN}	0.54	0.54
α_{sf} (1/m)	1770	1770
η (m^3/s)	0.60	0.54

Thermal management index of structure using Copper is greater than Aluminum. Due to higher conductivity of Copper, heat removed by the structure is greater as compare to Aluminum. Copper material is selected by considering the results shown in Table 5.

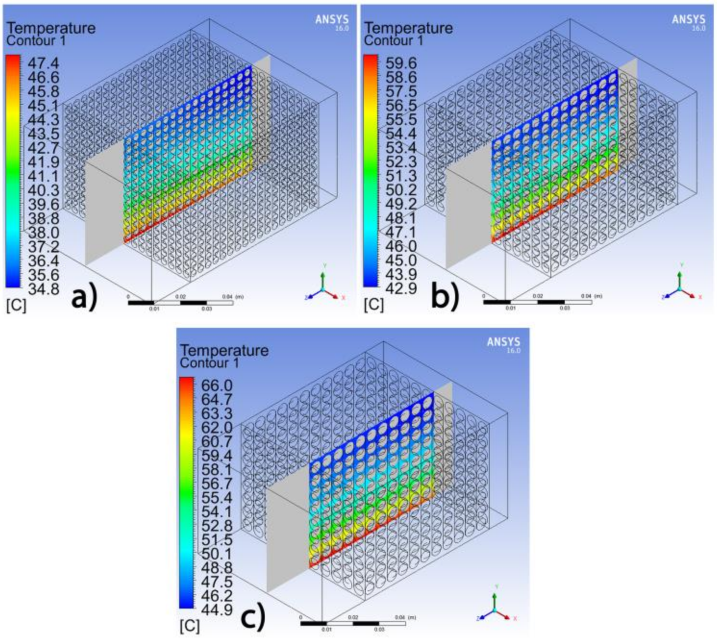

Fig. 3 Temperature distribution of; a) circularbore1, b) circularbore2, c) circularbore3

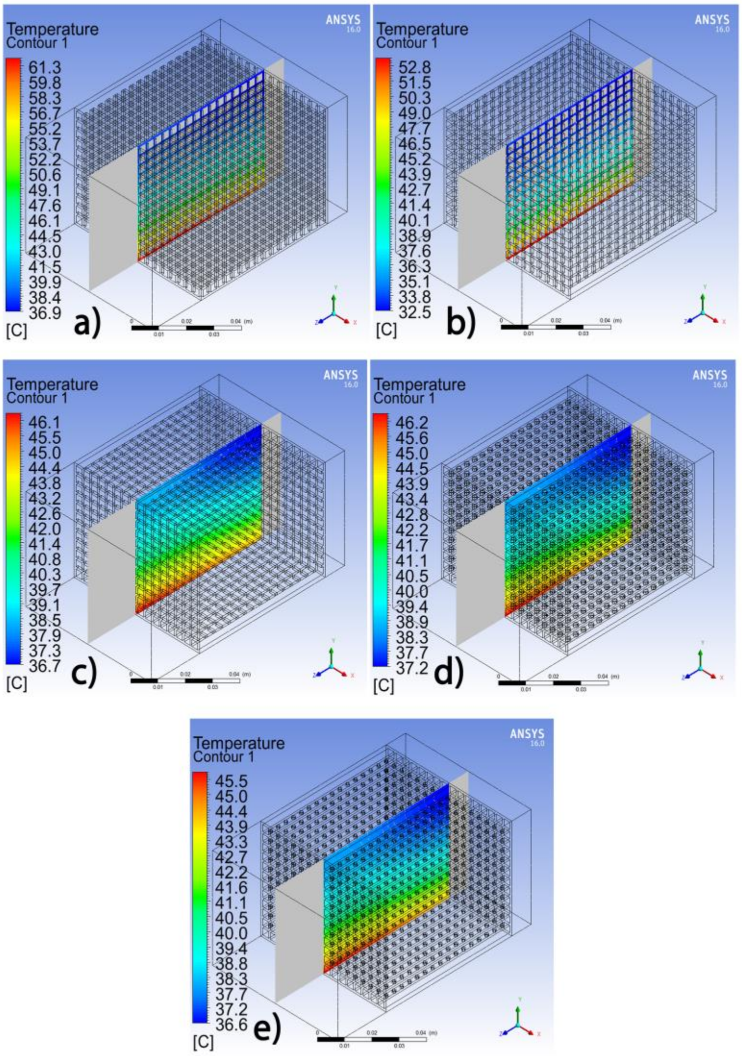

Fig. 4 Temperature distribution of; a) squarebore1, b) squarebore2, c) squarebore3 d) squarebore microhole1 e) squarebore microhole2

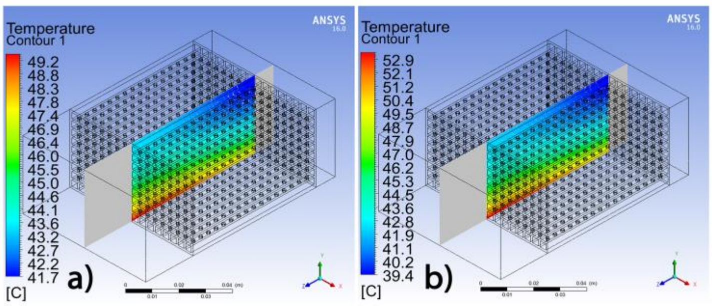

Fig. 5 Temperature distribution of; a) squarebore microhole3 (Cu), b) squarebore microhole3 (Al)

A YZ plane created in the mid of the solid-fluid domain shows the temperature distribution inside the structure. It can be viewed that temperature is higher at the base and then gradually start decreasing to the top of the structure. The maximum base temperature noted for circularbore1, circularbore2 and circularbore3 are 47.7^{0}C, 60^{0}C and 66.2^{0}C respectively as shown in the Fig. 3. The maximum base temperature noted for squarebore1, squarebore2, squarebore3, squarebore microhole1 and squarebore microhole2 are 62.4^{0}C, 53.7^{0}C, 46.6^{0}C, 46.7^{0}C and 46.2^{0}C respectively, as shown in the Fig. 4. The maximum base temperature noted for squarebore microhole3 (Cu) and square microhole3 (Al) was 49.7^{0}C and 54^{0}C respectively, as shown in the Fig. 5. The inlet face is directly facing the cool air coming from the fan that is the reason temperature is low at inlet as compare to the outlet face.

3. EXPERIMENTAL SETUP

After numerical study, we select squarebore microhole3 (Cu) structure as it is the optimal structure for heat dissipation media among all the structures discussed in this research work. We perform experiment on this selected structure and the obtained results are compared with numerical predictions. The optimized cellular structure is manufactured on the Wire Cut Electrical Discharge Machining (EDM) as shown in the Fig. 6.

Fig. 6 Fabricated squarebore microhole3 (Cu) structure

3.1. Test Loop

A constant heat is supplied to Copper block by DC electric iron heater which has been producing a heat flux of 35503W/m^2 continuously. A constant voltage of 210V and current of 0.71A is supplied to maintain the constant heat generation of 150W. Electric iron heater is connected to the AC to DC converter because a DC iron heater is operated. Copper block is mounted on the top of cellular structure for uniform distribution of the heat flux. All exposed surfaces are insulated by using fiberglass wool. In order to measure the base temperature, a fine wire K-type thermocouple is attached with the temperature meter, inserted between the heated copper block and the cellular structure. The outlet air temperature is measured by another K-type thermocouple. Set of data is obtained when steady state condition reached. Steady state is identified when the temperature measurements changed by no more than ±0.1^{0}C in 3 min. A DC fan with speed controller to supply inlet air at different velocities is attached to AC to DC converter. Anemometer is used to measure the inlet air velocity and a duct is used for the smooth passage of air flow. After the duct, cellular structure was placed. Schematic of experimental setup is shown in the Fig. 7.

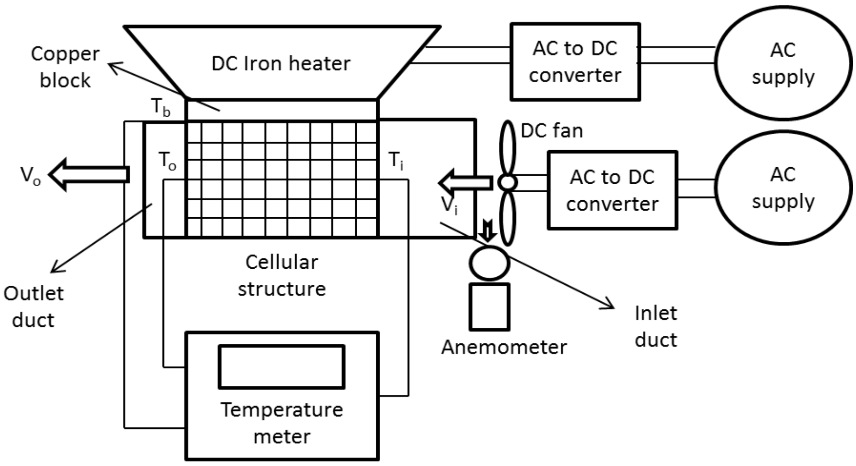

Fig. 7 Schematic of experimental setup

3.2. Uncertainty Analysis

The uncertainty in the experimental data is estimated by the method developed by Kline and McClintock [9]. This method incorporates the estimated uncertainties in the experimental measurement of heat transfer rate. The uncertainty in the heat transfer rate is found as 4.9%. The uncertainty related with the temperature measurements is estimated as $\pm 0.1^0$C.

4. RESULTS AND DISCUSSIONS

4.1. Effect of Pressure Drop and Pressure Loss Coefficient with Open Area Ratio

Open area ratio is basically the remaining area ratio of blockage ratio (1-R_{BR}). Blockage ratio is the ratio of frontal blocked area to the frontal total area. Variation of pressure drop with open area ratio is shown in the Fig. 8. The three structures (squarebore microhole1, squarebore microhole2, squarebore microhole3) offers the minimum pressure drop with almost maximum open area ratio at the inlet velocity of 6m/s. Maximum pressure drop was observed by circularbore1 structure with minimum open area ratio. Circularbore3 structure is showing lower pressure drop because of larger bore diameter, so air easily pass through. It is observed that circularbore1 offer 42.5% more pressure drop as compare to the squarebore2 through which we decided that squarebore structure is better than circularbore structure. Squarebore1 is a wire mesh structure that’s why shows greater pressure loss as compare to other the squarebore structures.

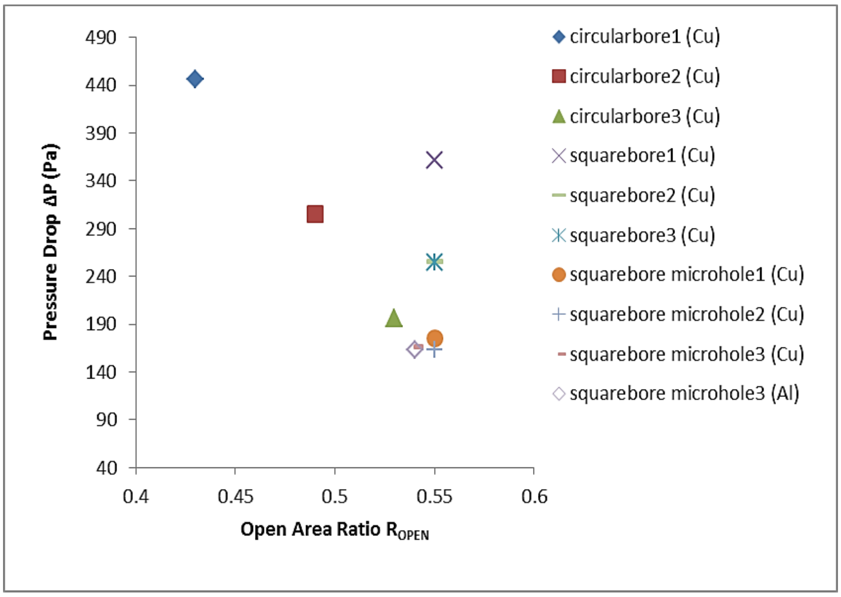

Fig. 8 Variation of pressure drop with open area ratio

Variation of pressure loss coefficient with open area ratio is shown in the Fig. 9. We observe the similar trend is of variation of pressure loss coefficient with open area ratio as reported by Tian et al. [10] for square and diamond shape cellular metal core panels in their Fig. 7. The pressure loss across a unit cell can be described by a single parameter R_{open} (or ε). The curve shows that the frontal area blockage causes large pressure loss that is why circularbore structures has large pressure loss coefficient as compare to squarebore structures. Circularbore3 (Cu) has large bore diameter that's why it shows less pressure loss coefficient.

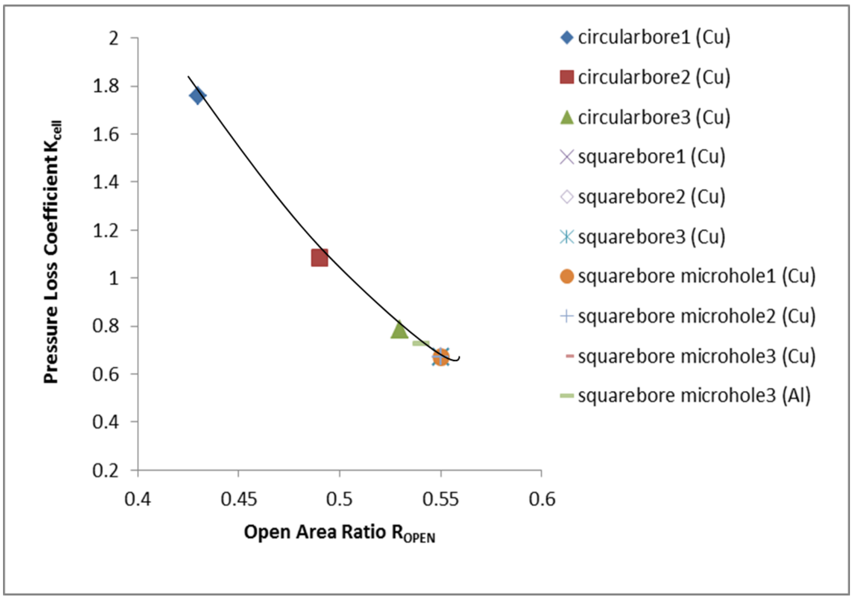

Fig. 9 Variation of pressure loss coefficient with open area ratio

4.2. Effect of Pressure Drop with Porosity

Porosity is obtained by subtracting the ratio of the volume of structure to total volume of the block from unity [1-(V/V_b)]. Higher porosity means less solid material per unit volume, and hence less conduction through the structure, while force convection will be greater. Lower porosity means less emptiness volume per unit volume, and hence less contribution of forced convection while conduction will be greater. Variation of pressure drop with porosity is shown in the Fig. 10. Squarebore1 structure depicts very high porosity because its structure is like a textile wire mesh, and hence its convection heat transfer is found maximum, but offering higher pressure drop. The structures (sqaurebore microhole1, squarebore microhole2, squarebore microhole3) provide less pressure drop as compare to the rest of all the structures discussed here.

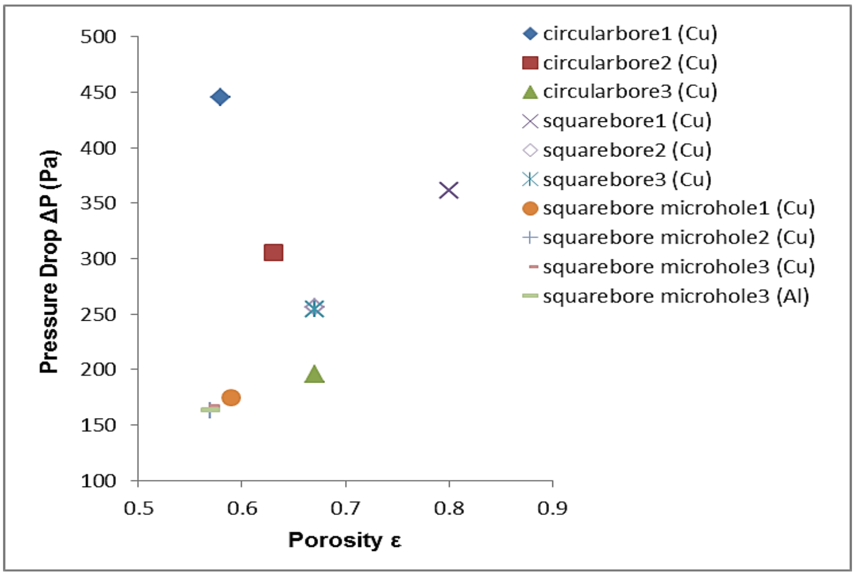

Fig. 10 Variation of pressure drop with porosity

4.3. Thermal management index

The thermal management index is the ratio of amount of heat dissipated from the structure to the pressure drop across the structure. More pressure drop across the structure requires more fan power to be supplied. Ultimate goal for designing of the best cellular structure is to dissipate the maximum amount of heat with minimum pressure drop across the structure. Thermal performance is evaluated for each of the cellular structure discussed in this research. The thermal management index η of all the cellular structures studied is shown in the Fig. 11. It can be seen from previous sections, that squarebore1 (Cu) is providing the maximum surface area density, but pressure drop across the structure is greater that is the reason its thermal management index η is 0.31, which is lesser than all the other squarebore structures. Maximum thermal management index η is noted for squarebore microhole2 (Cu) as 0.66 with structure height of 49mm, while the optimized structure squarebore microhole3 (Cu) has thermal management index η of 0.60 with structure height of 37mm. The optimized structure squarebore microhole3 shows thermal management index η of 0.60 and 0.54 by using Copper and Aluminum materials respectively.

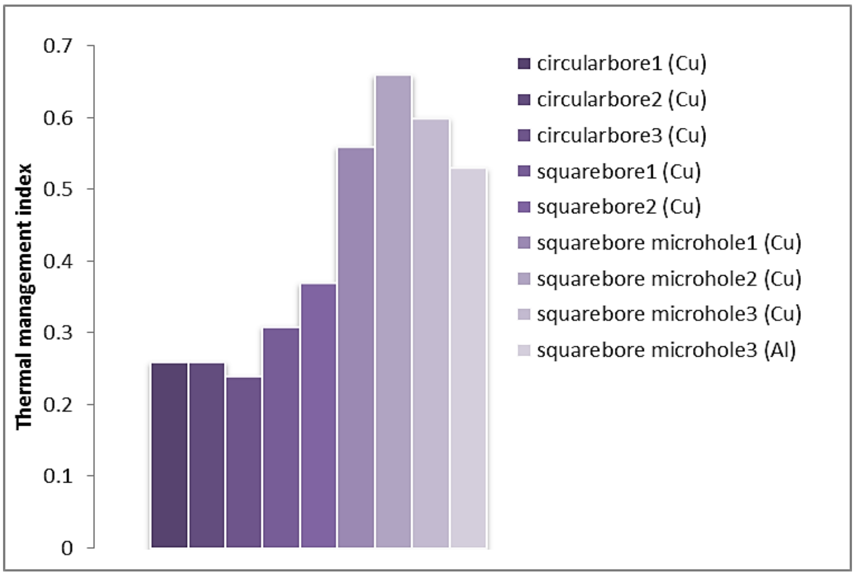

Fig. 11 Thermal management index

4.4. Effect of Heat Transfer Rate with Surface Area Density

High surface area densities are desirable for compact heat exchangers. A heat exchanger with α_{sf} >700m^2/m^3 is called a compact heat exchanger [10]. All of the structures studied in this research are compact heat exchangers as their surface area density (α_{sf}) are higher than 700m^2/m^3. Squarebore1 offers the maximum surface area density, which depicts the maximum heat transfer through convection is possible among rest of the structures discussed. Variation of amount of heat transfer rate with surface area density is shown in Fig.12. The amount of heat transfer by circularbore1 and squarebore1 is higher but pressure drop is estimated higher as shown in Fig. 8 and Fig. 9.

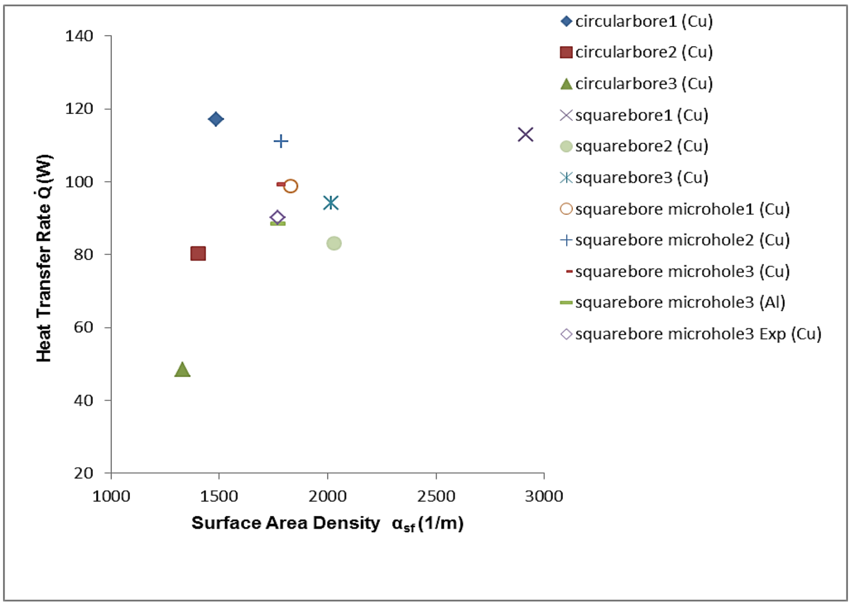

Fig.12 Variation of heat transfer rate with surface area density

4.5. Effect of Base Temperature with Surface Area Density and Inlet Velocity

Base temperature of electronic devices should not exceed 60-80^{o}C. Variation of base temperature with surface area density of all the structures studied in this research is shown in the Fig. 13. Circularbore structures offer the minimum surface area density which means that the less will be convection and more will be conduction. Maximum surface area density is offered by squarebore1 (Cu), which ensures the maximum convection heat transfer, but base temperature is very high as 62.4^{o}C, which means that it requires high inlet air velocity to remove the produced heat in the structure. The data depicts that base temperature of squarebore microhole3 (Cu) is 49.7^{o}C while the same structure with Aluminium material is at 54^{o}C, because thermal conductivity of Copper is 387.6W/mK while that of Aluminium is 202.4W/mK. Base temperature of squarebore microhole3 (Cu) calculated experimentally is 53.5^{o}C at air inlet velocity of 6m/s with 150W of heat generation. The experimental data is in good agreement with the numerical prediction as it shows 8.71% error calculated between the base temperature computed numerically and experimentally at 6m/s. It is than compared with the base temperature noted for rectangular mini-channel at 11.1m/s with 160W heat generation was 55^{o}C by Mohammed and El-Baky [1]. Base temperature noted by using water at 1.03m/s (1L/min) with 0.2mm fin spacing was 40.5^{o}C by Jajja et al. [2] while Base temperature noted using alumina nanofluid for 1% of volumetric concentration at 1L/min was 43.9^{0}C by Rafati et al. [8].

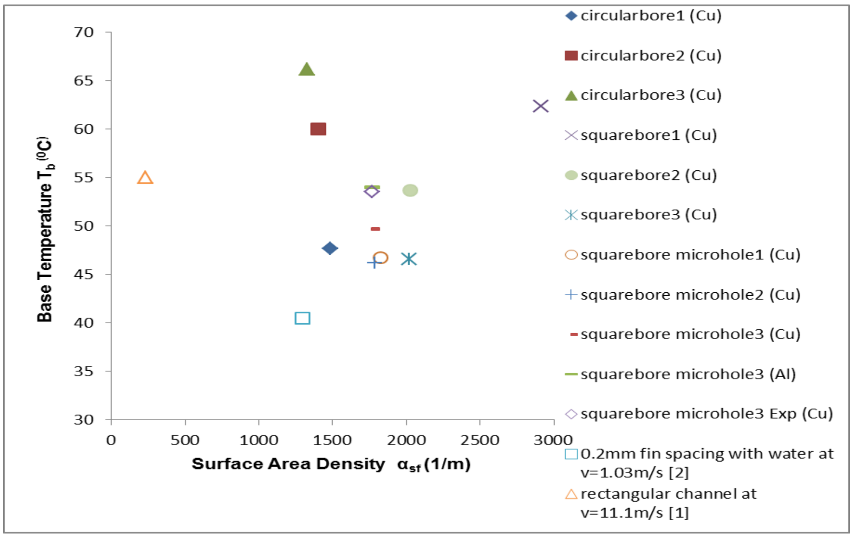

Fig. 13 Variation of base temperature with surface area density

Variation of base temperature with inlet velocity of the optimized structure is shown in the Fig. 14. The curve showing numerical results is slightly below the experimental curve with a difference of 3.8°C. We estimate an error of 8.71% between the numerical and experimental data. Base temperature tends to reduce with increasing the inlet velocity of air. The maximum base temperature of numerical and experimental data is noticed at the inlet velocity of 6m/s as 49.7°C and 53.5°C respectively, while the minimum value is attained at 10m/s as 43.6°C and 47.4°C respectively.

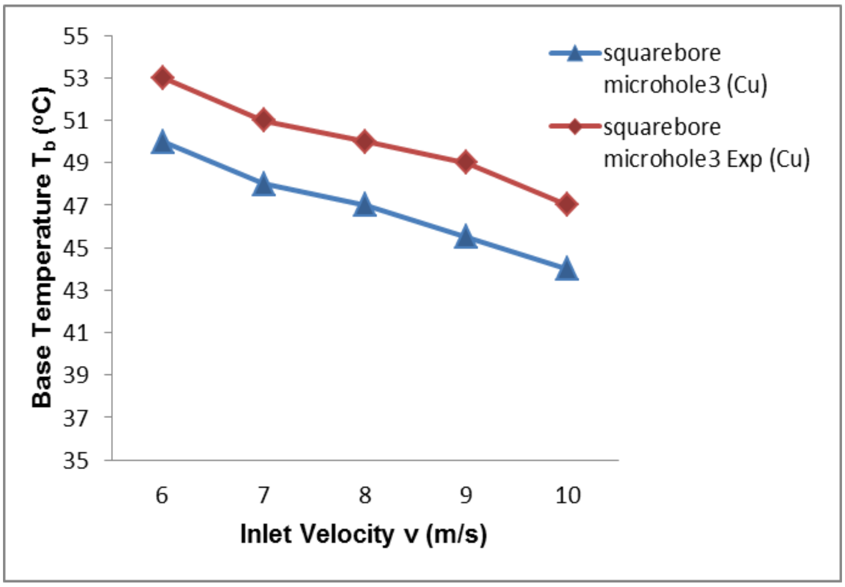

Fig. 14 Variation of base temperature with inlet velocity

5. Conclusion

Rapid development in the electronic technology has made researchers to find new modes to dissipate the heat generated timely to save the electronics chips. Nanofluids and water cool heat sinks are now in practice but require extra cooling mechanism for cooling of fluid. Thermo-mechanical properties of cellular structures are higher as compare to the metal foams. Therefore, cellular structures can provide better performance with acceptable base temperature and with very low pressure drop. In this research work it is observed that circularbore1 structure offer 42.5% more pressure drop as compare to the squarebore2 structure while the only difference is of square void cross section. The optimum structure was investigated as squarebore microhle3 among different structures discussed. Thermal management index η of squarebore microhole3 is 0.60 and 0.54 by using Copper and Aluminium materials respectively. The minimum base temperature for the optimized cellular structure estimated to be 43.6^0C and 47.4^0C numerically and experimentally respectively with inlet velocity of 10m/s and at heat flux of 35503W/m^2 (150W of heat supplied). The numerical results for the base temperature are in close agreement with experimental results with the error of 8.71%.

6. Bibliography

[1] Mousa M. Mohammed and Mostafa A. Abd El-Baky, "Air cooling of mini-channel heat sink in electronic devices," *Journal of Electronics Cooling and Thermal Control*, vol. 3, pp. 49-57, February 2013.

[2] Saad Ayub Jajja, Wajahat Ali, Hafiz Muhammad Ali, and Aysha Maryam Ali, "Water cooled minichannel heat sinks for microprocessor cooling: Effect of pin spacing," *Applied Thermal Engineering*, vol. 64, pp. 76-82, 2014.

[3] S. Gochman et al., "The Intel Pentium M processor: micro architecture and performance," *Int. Technol. J.*, vol. 7, pp. 21-36, 2003.

[4] M. F. Ashby et al., "Metal foams: A design guide, butterworth-heineman," , Boston, MA, USA, 2000.

[5] M. Kaviany, *Principles of heat transfer in porous media springer*. New York, 1995.

[6] A. G. Evans, J. W. Hutchinson, N. A. Fleck, M. F. Ashby, and H.N.G. Wadley, "The topological design of multifunctional cellular metals," *Prog. Mater. Sci.*, vol. 46, pp. 309-327, 2001.

[7] J. Tian et al., "The effects of topology upon fluid-flow and heat transfer within cellular copper strucutres," *International Journal of Heat and Mass Transfer*, p. 16, 2004.

[8] M. Rafati, A A Hamidi, and M. S. Niaser, "Applications of nanofluids in computer cooling systems (heat transfer performance of nanofluids)," *Applied Thermal Engineering*, vol. 45-46, pp. 9-14, 2012.

[9] S. J. Kline and F. A. McClintock, "Describing uncertainties in single-sample experiments," *Mech. Eng.*, vol. 75, pp. 3-8, 1953.

[10] J. Tian, T. J. Lu, H. P. Hodson, D. T. Queheillalt, and H.N. G. Wadley, "Cross flow heat exchange of textile cellular metal core sandwich panels," *Journal of Heat and Mass Transfer*, vol. 50, pp. 2521-2536, March 2007.

[11] C. Zhao, "Review on thermal transport in high porosity cellular metal foams with open cells," *Int. J. Heat Mass Transfer*, vol. 55, pp. 3618-3632, 2012.

[12] T.J.Lu, "Ultralight porous metals:from fundamentals to applications," *Acta Mech. Sin.*, vol. 18, pp. 457-479, 2002.

[13] S. Gu, T.J. Lu, A.G. Evans, "On the design of two-dimensional cellular metals for combined heat dissipation and structural load capacity," *Inter. J. Heat Mass Transfer*, vol. 44, p. 2163, 2001.

[14] Yunus A. Cengel, *Heat and mass transfer*, 3rd ed.: Mcgraw-Hill (Tx), 2002.

[15] A. F. Bastawros, A. G. Evans, and H. A. Stone, "Evaluation of cellular metal dissipation media," *Technical Report MECH*, 1998.

[16] S. Mancin, C. Zilio, A. Diani, and L. Rossetto, "Experimental air heat transfer and pressure drop through copper foams," *Exp. Therm. Fluid Sci.*, vol. 36, pp. 224-232, 2012.

[17] H. Zhang, L. Chen, Y. Liu, and Y. Li, "Experimental study on heat transfer performance of lotus type porous copper heat sink," *International Journal of Heat and Mass Transfer*, vol. 56, pp. 172-180, 2013.

[18] A. Bhattacharya and R. L. Mahajan, "Finned metal foam heat sinks for electronics cooling in forced convection," *J. of Electronic Packaging*, vol. 124, pp. 155-163, 2002.

[19] T.J. Lu, "Heat transfer efficiency of metal honeycombs," *Int. J. Heat Mass Transfer*, vol. 42, pp. 2031-2040, 1999.

[20] T. J. Lu, H. A. Stone, and M. F. Ashby, "Heat transfer in opencell metal foams," *Acta Mater*, vol. 46, pp. 3619-3635, 1998.

[21] J. Hwang, G. Hwang, R. Yeh, and C. Chao, "Measurement of interstitial convective heat transfer and frictional drag for flow across metal foams," *J. Heat Transfer*, vol. 124, pp. 120-129, 2002.

[22] C. T. DeGroot, A. G. Straatman, and L. J. Betchen, "Modeling forced convection in finned metal foam heat sinks," *Journal of Electronic Packaging-Transactions of the ASME*, vol. 131, 2009.

[23] C. Y. Zhao, T. Kim, T. J. Lu, and H. P. Hodson, "Modeling on thermal transport in celleular metal foams," *J.Thermofluid Phys.(in press)(also in:8th Joint AIAA/ASME Thermophysics and Heat Transfer Conference,AIAA*, June 2002.

[24] H. Seyf and M. Layeghi, "Numerical analysis of convective heat transfer from an elliptic pin fin heat sink with and without metal foam insert," *J. Heat Transfer*, vol. 132, 2010.

[25] J. Tian et al., "The effects of topology upon fluid-flow and heattransfer within cellular copper structures," *Int. J. Heat Mass Transfer*, vol. 47, pp. 3171-3186, 2004.

[26] S. Y. Kim, J. W. Paek, and B. H. Kang, "Thermal performance of aluminum foam heat sinks by forced air cooling," vol. 26, pp. 262-267, 2003.

[27] W. Lu, C. Zhao, and S. Tassou, "Thermal analysis on metal foam filled heat exchangers Part I: metal-foam filled pipes," *Int. J. Heat Mass Transfer*, vol. 49, pp. 2751-2761, 2006.